Journal of Physics: Condensed Matter **XX** (XXXX) XXXXXX https://doi.org/XXXX/XXXX

Journal of Physics: Condensed Matter **XX** (XXXX) XXXXXX https://doi.org/XXXX/XXXX

Electrochemical scanning probe analysis used as a benchmark for carbon forms quality test

Gianlorenzo Bussetti[1], Rossella Yivlialin[1§*], Franco Ciccacci[1], Lamberto Duò[1], Eugenio Gibertini[2], Alessandra Accogli[2], Ilaria Denti[2], Luca Magagnin[2], Federico Micciulla[3], Antonino Cataldo[3], Stefano Bellucci[3], Alexander Antonov and Inna Grigorieva[4]

[1] Department of Physics, Politecnico di Milano, Milano, Italy
[2] Department of Chemistry, Materials and Chemical Engineering "Giulio Natta", Politecnico di Milano, Milano, Italy
[3] INFN-Laboratori Nazionali di Frascati, Roma, Italy
[4] Optigraph GmbH, Berlin, Germany

[§] current affiliation: Institute for Solar Fuels, Helmholtz-Zentrum Berlin für Materialien und Energie GmbH, Berlin, Germany

[*]E-mail: rossella.yivlialin@helmholtz-berlin.de

Received xxxxxx
Accepted for publication xxxxxx
Published xxxxxx

Abstract

Carbon forms (graphite, pyrolitic graphite, highly oriented pyrolytic graphite, glassy carbon, carbon foam, graphene, bucky paper, etc.) are a wide class of materials largely used in technology and energy storage. The huge request of carbon compounds with reliable and tunable physical and chemical properties is tackled by contriving new production protocols and/or compound functionalizations. To achieve these goals, new samples must be tested in a trial-and-error strategy with techniques that provide information in terms of both specimen quality and properties. In this work, we prove that electrochemical scanning probe techniques allow testing the performances of carbon compounds when are used as an electrode inside an electrochemical cell. Comparing the results with a reference sample (namely, highly oriented pyrolitic graphite, HOPG) gives an insight on defects in the specimen structure, performances and possible applications. In this study, we concentrate on traditional carbon forms already employed in many fields versus new specimens produced by Optigraph GmbH, in view of possible applications to the field of energy storage.

Keywords: graphite intercalated compounds, HAPG, pyrolytic graphite, electrochemical SPM

1. Introduction

Carbon forms (namely, graphite, pyrolitic graphite, higly oriented pyrolitic graphite (HOPG), glassy carbon, graphene, multi-layered graphene, nanotubes, nano-pellets, buckypaper, carbon foam, etc.) are considered of strategical importance in many fields. Graphite and glassy carbon are employed as electrodes in electrochemical cells and/or in new batteries [1-6]; graphene (Gr) and multi-layered Gr sheets are exploited in, *e. g.*, supercapacitors [7] anticorrosive coatings [8] and green energy applications [9]; nanotubes are used for their exceptional transport [10] and mechanical [11] properties and possible application in biomedicine [12]; carbon nanopellets show promising results for natural gas storage

[13]; carbon buckypaper is studied for enhancing thermoelectric performances [14] or catalytic processes [15]; finally, carbon foam is also used in military applications being an excellent electromagnetic shield [16]. As a consequence, the technological, strategical and economical interest in producing new carbon forms is continously expanding in terms of functionalization, tuning their properties and finding new strategies to reduce the time-preparation protocols. In order to achieve these goals, the physical and chemical characterization of the new carbon forms is mandatory. The new specimen properties are generally studied by optical techniques [17], photoelectron spectroscopies [18], diffraction [19], scanning probe microscopy [20] and electrochemistry [21] among others.

In this work, we propose a complementar investigation for carbon forms where the specimen undergoes a peculiar electrochemical process. The Faradaic current intensity behaviour, together with the sample surface evolution, are monitored. This approach requires two basic preconditions: i) an experimental set-up, where scanning probe microscopy (SPM) is coupled with electrochemistry; ii) a reference for both samples and EC treatments to ensure a clear interpretation of the EC process applied to all the other carbon forms. Issue (i) can be fullfilled by the so-called EC-SPM [namely, EC-atomic force microscopy (EC-AFM) and EC-scanning tunneling microscopy (EC-STM)] [22,23]. These techniques are optimized for acquiring microscopic images with probes directly immersed inside the electrolytes without any contamination or influence in the EC characterization (*e. g.*, by cyclicvoltammetry, see below). The second issue is more critical to accomplish: the EC reaction selected for the study has to, on the one hand, produce clear effects on carbon compounds while, on the other hand, present a clear interpretation, in order to get reliable information on the properties of the new carbon specimen. The authors have experience on the HOPG anion intercalation, occuring when graphite is biased in acid electrolytes. We have acquired data on the role played by the electrolytes [24], the temperature and the time effects [25,26], the electrolyte pHs [27], the structure [28] and the morphological [29] evolution of the HOPG electrode surface and paved the way to a first investigation of the buried graphite layers [30]. Finally, we succeeded in refining the current interpretation model of the involved chemical reaction [31]. In acid electrolytes, such as diluted sulfuric acid (H_2SO_4, 1 M), solvated anions are able to intercalate in the stratified HOPG structure as soon as a positive bias is applied to the electrode [26]. HOPG becomes a so-called graphite intercalated compound (GIC) where graphite layers are alternated with solvated anions [32]. When the oxygen evolution reaction (OER) potential is applied to the graphite electrode, the latter undergoes the following chemical reaction:

$$C_x + A^- + y(H_2O) \rightarrow C_x^+y(H_2O)A^- + e^- \quad (1)$$

A reaction of a certain amount of carbon atoms (C_x) with the solvated anions (A) occurs at any buried layer where the intercalation process takes place. The process also develops gases (namely CO, CO_2, O_2), which swell the graphite basal plane forming blisters on the electrode surface [33].

The described process was initially studied through EC characterizations. Among various EC techniques, cyclic voltammetry (or CV, consisting in the measurement of the Faradaic current flowing through the electrode as a function of the applied potential) shows a voltammogram with characteristic features (indicated by the arrows in **Figure 1**).

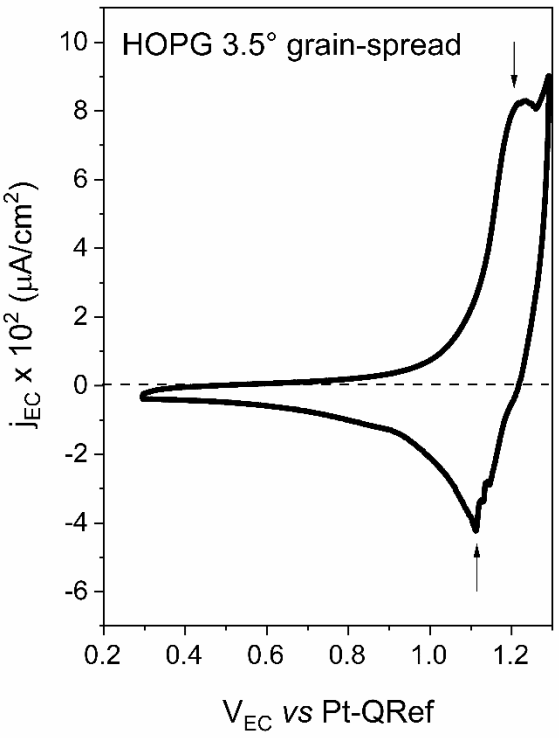

Figure 1. Typical CV of the HOPG 3.5° grain-spread sample. Scan rate = 25 mV/s.

Typically, the shoulder visible in the anodic part of the CV represents the fingerprint of the anion intercalation while the negative (cathodic) peak is traditionally interpreted in terms of a partial de-intercalation process [28,29]. These ascriptions were furthermore confermed by EC-AFM investigations, which consist in monitoring the electrode evolution *in-situ* and in real time [34]. In particular, the HOPG surface blistering can be detected by the EC-AFM, as showed in **Figure 2**: instead of the well-known graphite morphology, characterized by steps and flat terraces on the overall surface (see panel a), rounded 3D structures appear in

the topograpy image (b), which prove that reaction (1) took place.

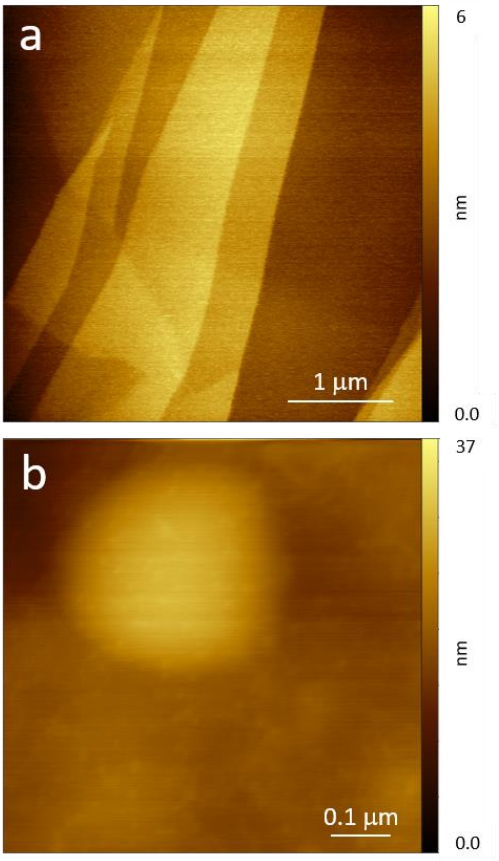

Figure 2. AFM topography images of 3.5°grain-spread HOPG. a) pristine sample, b) post EC acid-treatment.

The interpretative model for blisters described above foresees the two main CV features to be related to specific microscopic processes (intercalation and de-intercalation, respectively), which can only occur in the stratified structure of the graphite crystal. Consequently, the CVs acquired on those carbon forms that are not suitable for a microscopic investigation, due to their high surface roughness (*e. g*., carbon foam and pyrolitic graphite), disclose important information when their cyclic-voltammograms are compared to Figure 1. However, when it is possible to conduct the microscopic analysis at applied positive EC bias, the evolution of the electrode surface contains details on the quality of the specimen structure and can be direcly compared to the one of HOPG. Considering these facts, the anion intercalation mechanism represents the proper chemical reaction for testing different carbon forms.

Our work reports the investigation of the anion intercalation process into three distinct carbon forms classes: 1) samples available from a specialized factory (namely Optigraph GmbH) in the graphite production; 2) a special electrode prepared in lab (buckypaper of Graphene_NanoPlatelets (GNPs)) and (3) other specimens available from the market (graphite, glassy carbon and carbon foam). Regarding the first class, Optigraph provided HOPG samples of different grade, namely both ZYH (mosaic spread 3.5°) and ZYA (mosaic spread 0.4°), as well as new specimens such as HOPG flex, highly aligned pyrolytic graphite (HAPG), pressed thermal conductive pyrolytic graphite (TPG), and special samples suitable for the analysis of the crystal edges (see below for details). Our test strategy is applicable to almost all of these cases and we will discuss the different sample behaviors in the following lines.

2. Materials and Methods

A commercial EC-AFM (Keysight 5500) was used for the sample analysis. This instrument controls the electrochemical process through a potentiostat that can measure the Faradaic current, with a range from pA to mA. The sample, which represents the working electrode (WE), is placed in a three-electrode cell, where a Pt wire is used as a counter electrode (CE). A second Pt wire is exploited as a reference. The latter represents a quasi-reference (PtQRef) [35], with a stable (within few mV) shift of + 0.74 V with respect to the standard hydrogen electrode (SHE), when immersed in acid electrolytes [28]. In some cases (edge graphite samples from Optigraph), the specimens could not be clamped tightly so that a different EC configuration was necessarely adopted, employing a custom-made Teflon sample holder that exposes the sample surface through a circular window (1 cm^2). Again, Pt wires were used as counter and quai-reference electrode.

The 5500 EC-AFM allows the immersion of the scanner head inside the electrolyte. Si-tips, mounted on gold or aluminum coated cantilavers, were used in this investigation. Depending on the sample mechanical characteristics and surface roughness, the image acquisition was performed either through contact or tapping mode. We did not observe significant morphological differences after the EC treatment between the samples observed *in-situ* and and those ones studied *ex-situ*.

A water-diluted (0.5 or 1 M) H_2SO_4 solution was prepared as an eletrolyte and de-aerated by bubbling pure (5.5 grade) Ar for several hours.

The samples (25 × 25 × 1 mm^3) were used without any other further cleaning.

Several different types of Pyrolytic Graphite (PG) were provided by Optigraph. All types of PG were prepared by high temperature annealing from the same initial material - Pyrolytic Carbon. The difference in the annealing condition led to a different structure and properties of the PGs under investigation.

In HAPG, HOPG and HOPG-flex the grains are well aligned in the direction of the C-C-plane with mosaic spread below 1°. The samples consisted in plates of 25 × 25 ×1 mm^3 size with the main surface parallel to the basal plane

(orthogonal to the stacking direction of the graphene layers). The so called "edge samples", similar three PG types of 25 × 3 × 3 mm^3 size, are also present. In these samples both the surface, parallel to the basal plane, and the edge surface, consisting of crystallite edges and perpendicular to the basal plane, are of the same size.

In order to prepare the samples from TPG, the material was grained in an activation mill, and then the powder was pressed in a metal matrix at room temperature without any additional additives. The particles alignment is similar to the initial mosaic spread of this material, which is about 10°. Two types of samples 25 ×25 × 2 mm^3 size presented particles aligned along the main surface and particles perpendicular to this surface.

GNPs bukypaper is made by a filtration system of a solution of isopropylic alchool and GNPs and then pressed by using a Constant Pressure System [36], loaded with a force of 700 N. GNPs were synthezied starting from commercial intercalated graphite (provided by Asbury®) and they were expanded in a worm-like shape by using a short thermal treatment. The samples were then separated in graphene nanoplatelets by an ultra-sound bath [37, 38].

3. Results and Discussion

i) Optigraph samples

The first analysis is focused on understanding the role of the HOPG crystal structure. Traditionally, ZYH-grade (or AGraphH-grade) samples, where the grain disalignment (mosaic spread) is 3.5 ± 1.5°, are used to analyze the graphite intercalation. The studied HOPG samples are characterized by a smaller disalignment of 0.4 ± 0.1° (AGraphZ -grade). In **Figure 3**, we show subsequent CVs acquired on these high-quality specimens.

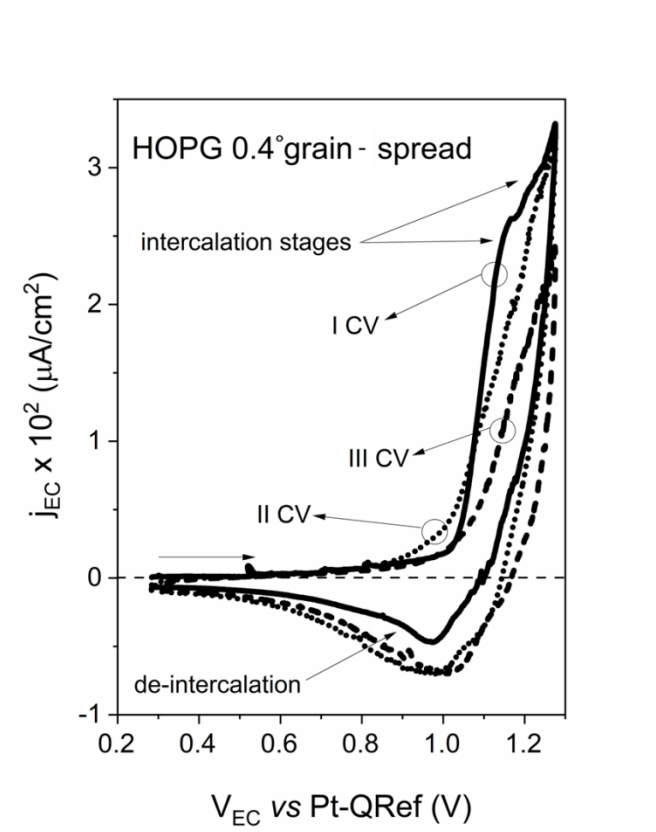

Figure 3. 3 subsequent CVs of the 0.4° grain-spread HOPG samples. Scan rate = 25 mV/s.

The reported voltammograms show the typical features observed on ZYH-grade HOPG (see Figure 1). Their interpretation is thus the same discussed in the Introduction. The intensity reduction of the anodic features during the subsequent cycles are interpreted in terms of a progressive filling of the inter-layer space inside the crystal. **Figure 4** reports the morphological analysis.

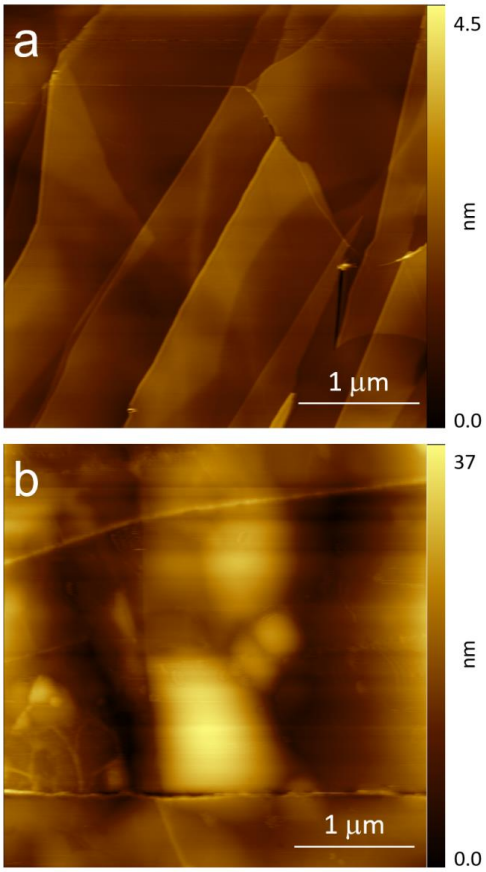

Figure 4. AFM topography images of the 0.4°-grain spread HOPG. a) pristine sample, b) post EC acid-treatment.

Panel a shows different flat terraces with multi-atomic step edges. After the CVs, the graphite basal plane is swollen (blisters), in close comparison with results reported in Figure 2. Regardless of the quality grade, HOPG samples undergo the same electrochemical process: anion intercalation (see the CV anodic shoulders and the cathodic peak that ensures a partial de-intercalation of species from the graphite layers) and blister evolution.

Some differences are observed for other PG samples. HOPG-flex was prepared according to the same procedure of standard HOPG, but the annealing condition such as time, temperature and deformation conditions were different. The result is a much softer material that could provide flexible films. The structural investigation showed that the material had fewer defects and a larger grain size compared to HOPG. In HOPG, the grain boundaries are decorated with relatively wide defect regions clearly visible by an acoustic microscope. In HOPG-flex the grain boundaries are acoustically transparent [40]. Different structure leads to specific material behaviour.

Figure 5 shows the collected CVs for the HOPG-flex. In this case, only the first CV recalls those collected in traditional HOPG samples. Starting from the second CV, it is not possible to intercalate any other solvated anion (absence of anodic features) and no de-intercalation cathodic peak is observed. A reduced amount of defects precludes the possibility of intercalation (see the maximum flowing current with respect to the HOPG in Figure 3).

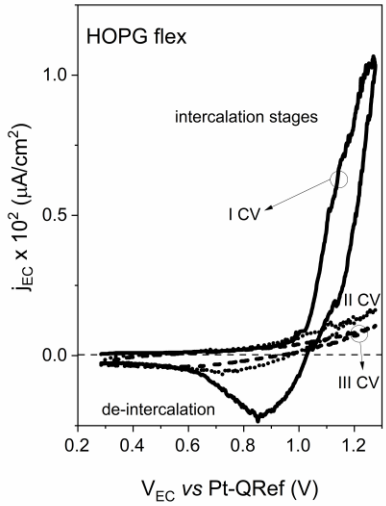

Figure 5. 3 subsequent CVs of the HOPG-flex sample. Scan rate = 25 mV/s.

This scenario is confirmed by the morphological analysis reported in **Figure 6**.

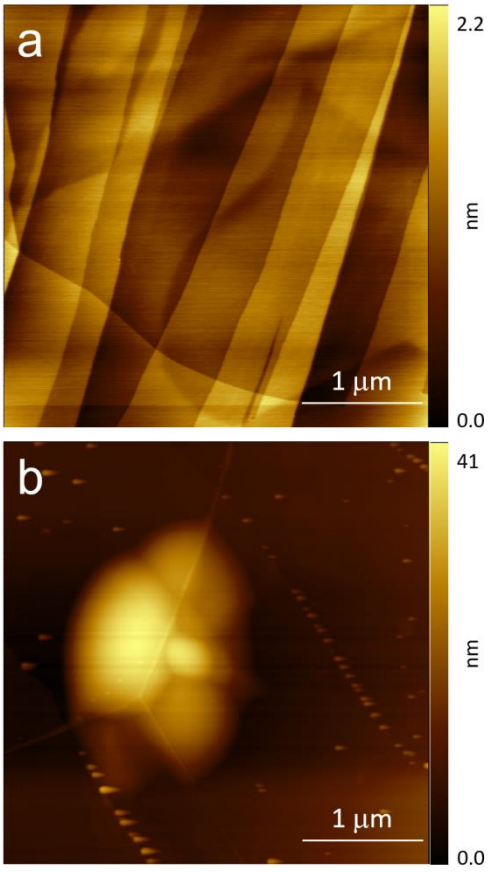

Figure 6. AFM topography images of the HOPG-flex sample. a) pristine sample, b) post EC acid-treatment.

The pristine specimen shows flat terraces as those observed in the HOPG reference/commercial sample. However, after the CV treatments, the basal plane is not as damaged as the one of the commercial HOPG (see Figure 4), where blisters cover all the graphite surface. In the case of the HOPG-flex, blisters are visible only close to steep step edges, *i. e*., where solvated anions have the possibility to enter inside the graphite crystal. In the other areas, flat terraces are well-visible. In Figure 6, small 3D structures are also visible along the step edges, which reasonably consist of some residuals from the original graphite terraces, created as a consequence of carbon dissolution in acid [28] and re-deposition of the surface after the extraction of the sample from the EC cell.

The evolution of the electrode surface completely changes for HAPG. HAPG is also a variant of the well-aligned PG as well as the two HOPGs discussed above. But the annealing technology is completely different, although it is also stress annealing at temperatures near 3000° C. A deeper improvement in the structure leads to a material with more flexible films and an even lower level of defects than the HOPG-flex case study [41, 42]. The structure of HAPG is closer to the ideal one, which is also confirmed by a smaller interlayer distance of 3,354 Å compared to 3,356 and 3,358 Å of HOPG-flex and HOPG, respectively. We report the collected CVs in **Figure 7**.

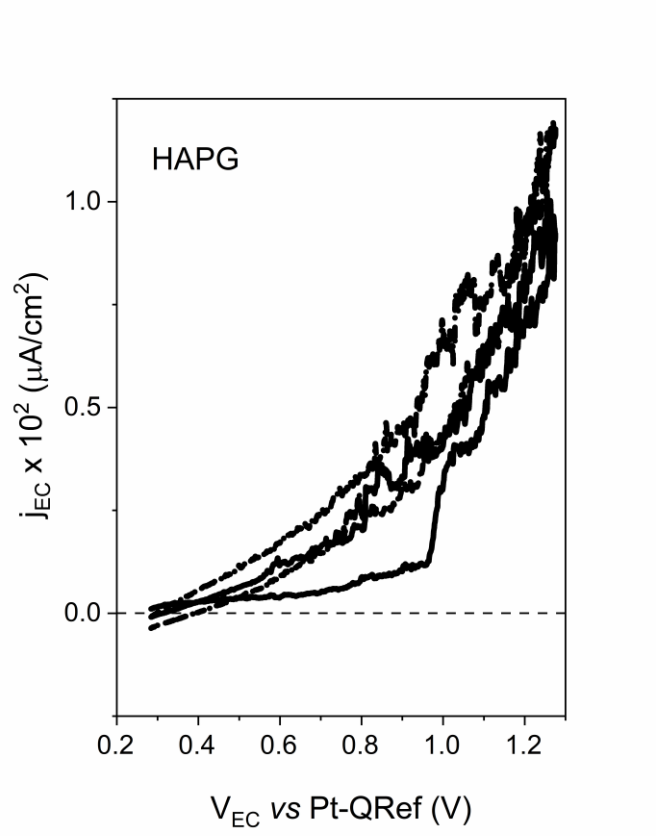

Figure 7. 3 subsequent CVs of the HAPG sample. Scan rate = 25 mV/s.

The electrochemical analysis of HAPG in sulfuric acid does not show any intercalation feature, neither cathodic Faradaic currents. It seems that no solvated anions are able to percolate inside the electrode crystal. The subsequent CVs are superimposed one to the other and the overall behavior mimics the one of an ideal electrode working close to the oxygen evolution reaction (OER). The morphological evolution is also significantly changed. In **Figure 8**, we report a representative AFM image. The pristine sample is characterized by very wide flat terraces, with steps almost parallel and well-aligned along the same direction. After the EC treatment, AFM reveals numerous clusters showing different behaviour with respect to the traditional blisters, both for the lateral and the vertical size. The electrode surface appears as melted as after an intense carbon dissolution caused by the acid electrolyte. In this case, clusters are ascribed as residuals of the dissolved original terrace.

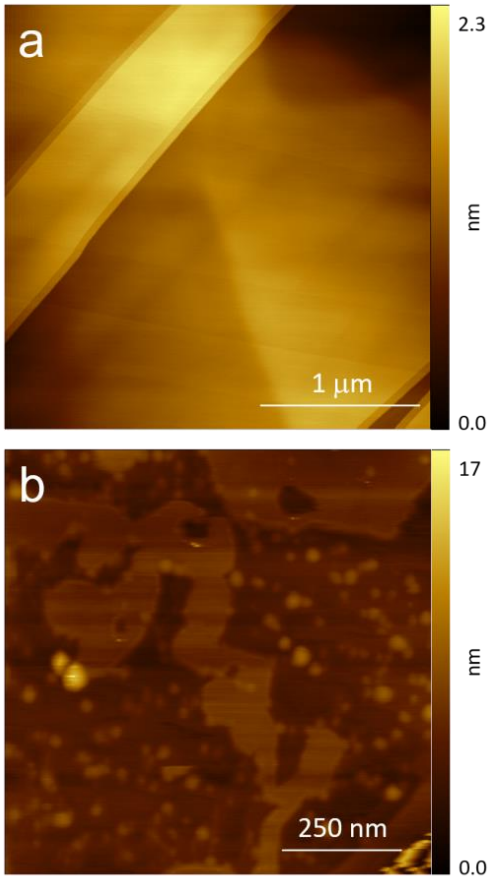

Figure 8. AFM topography images of HAPG. a) pristine sample, b) post EC acid-treatment.

Furthermore, TPG is a version of PG with a perfect crystalline structure, but obtained by annealing without external stress. Due to the absence of stress, the mosaic spread of the material remains quite high – about 10°. At the crystallites level, the material has a perfect structure close to HAPG.

Activation milling induces cleavage steps and dislocation (that is revealed in an increase of rhombohedral phase) which rises the activity of the material in the intercalation reaction. However, the milling process does not amorphize the graphite structure.

Pressing the powder allows to manufacture samples of any shape, which could be useful for electrochemical research and application. Due to structural features, perfect graphites, such as HOPG and HAPG, are mainly available as plates of 1 - 2 mm thick with the main surface parallel to the basal plane. For electrochemical experiments, the opposite orientation is required: the extent of the surface parallel to basal plane is less or equal to the edge surface.

Grinded TPG was pressed in metal mould at room temperature. The samples are prepared by applying different preassure loads that change the sample density. In our experiments, the sample density ranges whithin 1.55 (i) and 2.11 g/cm^3 (ii). We report and comment only these extreme cases. The CVs of the i-sample are reported in **Figure 9**.

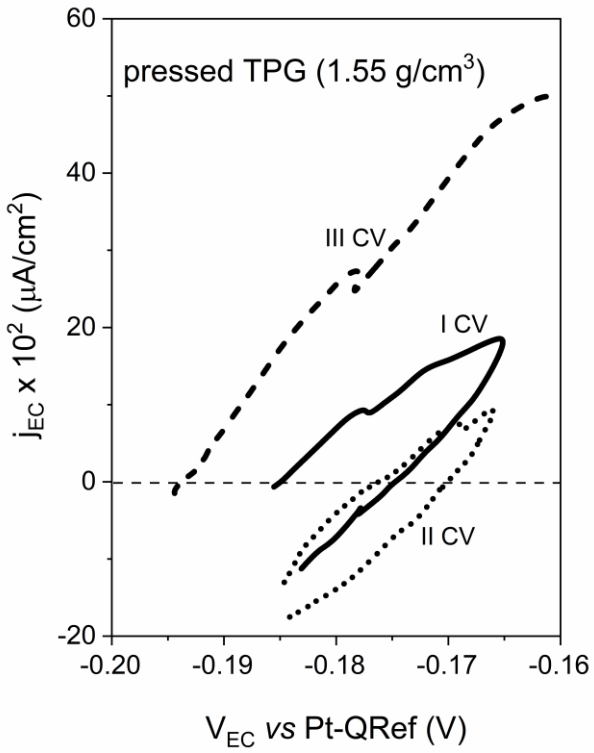

Figure 9. 3 subsequent CVs of the pressed TPG 1.55 g/cm^3 sample. Scan rate = 25 mV/s.

The CVs are completely different with respect to the previous cases. The EC potential (which measures the anodic current) is now slightly negative. The flowing current is order of magnitudes higher with respect to the characteristic values observed for HOPG. A significant current intensity shift is also observed when performing subsequent CVs. This behaviour suggests that the electrode is not stable and probably affected by a strong detriment that can contaminate the electrolyte and produce a current enhancement. In such conditions it is not possible to recognize blisters on the electrode surface. The AFM investigation, reported in Figure 10, confirms this interpretation.

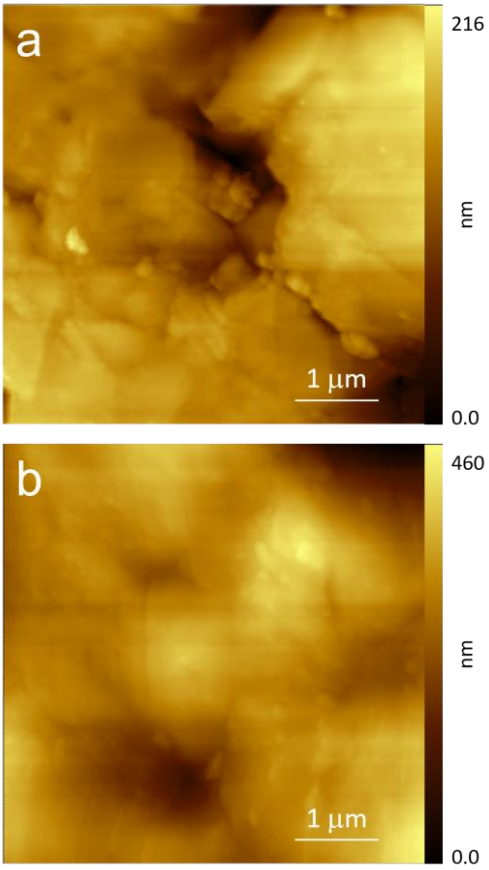

Figure 10. AFM topography images of 1.55 g/cm^3-TPG. a) pristine sample, b) post EC acid-treatment.

The pristine sample is rough and no clear structures are discernible. Reasonably, the electrode surface presents many fractures, defects, holes, etc., where solvated anions can pass through. After the voltammetries, the TPG surface appears swollen (see the color gradient values) but no clear features (blisters) are discernible. Moreover, the reduced contrast the AFM image has suggests a strong interaction with the electrolyte.

The results collected for the pressed TPG with a density of 2.11 g/cm^3 are reported below. The acquired CVs are shown in **Figure 11**. The instability of the voltammetries is also verified here. The III CV shape is clearly associated to a detriment of the electrode surface. However, we observe that I and II CVs show an anodic current enhancement that recalls the one of the HOPG electrodes close the OER in HOPG. Besides the very different line shapes of the CVs, we report a considerable shifting of the EC potential towards positive values. The higher sample density plays a reasonable role in reducing the number of entrance sites on the electrode surface with respect to the previous case. The crystal quality and the EC behavior of the HOPG electrode in acidic media are not reached, but the qualitative resemblance due to a higher preassure load used to prepare this TPG specimens is indisputable.

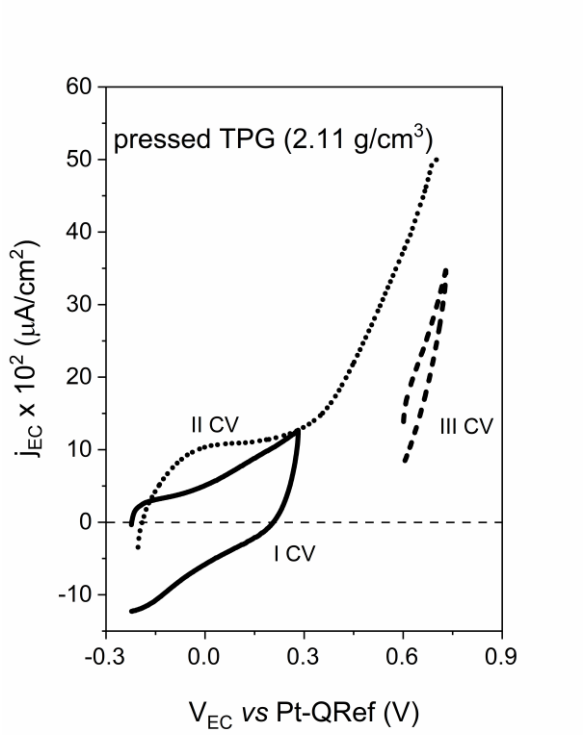

Figure 11. 3 subsequent CVs of the pressed TPG 2.11 g/cm^3 sample. Scan rate = 25 mV/s.

The morphological analysis is presented in **Figure 12**.

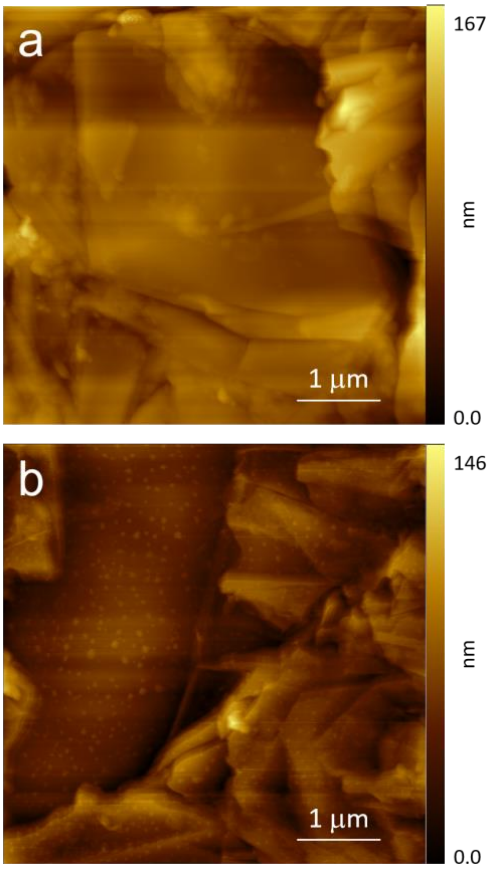

Figure 12. AFM topography images 2.11 g/cm^3-TPG. a) pristine sample, b) post EC acid-treatment.

The pristine sample is characterized by quite wide regions similar to terraces in the HOPG. Although the surface roughness is higher than in graphite (see the vertical color bar), the morphological investigation highlights the central role of the TPG density in the EC and microscopic behavior of the specimen. It is worth noting that, after the CV treatments, terraces are still visible and clusters appears on the surface. As already observed, the cluster could be composed by some electrolyte residuals after the extraction of the sample from the EC cell.

It is evident from these results that important information on the quality of the specimen can be deducted from the first CV, *i. e.*, before serious damage of the electrode surface occurs and then confirmed by the AFM investigation.

Finally, we explored the role of crystal edges in the intercalation process. In samples where the treated surface is parallel to the basal plane, the intercalate agent must first diffuse into the sample through atomic steps, grain boundaries and other defects on the sample surface [41]. Thus, diffusion can be a limiting step. To prove this point, "edge samples" of all three well aligned PG, were tested.

It is not possible to perform *in-situ* and real time experiments with these specimens. In fact, the sample cannot be clamped below the EC cell used in the Keysight 5500 system otherwise the preassure of the clamp accidentally clevages the crystal. For this reson, we acquired voltammetries by inserting the sample into the custom-made Teflon sample described in the Materials and Methods paragraph. The correposponding cyclic voltammetries are reported in **Figure 13**.

It is very interesting to compare the results in Figure 13 with the results in Figures 5, 6, 7. For standard samples, the most active material is HOPG, the intercalation in HOPG-flex is not so fast and the maximum current is three times less than for HOPG. When the electrolite remained in direct contact with edge surface, the ratio is the opposite: HOPG-flex is much more active than HOPG. HAPG also shows typical voltammogram with intercalation/de-intercalation features and demostrates to be more active than HOPG.

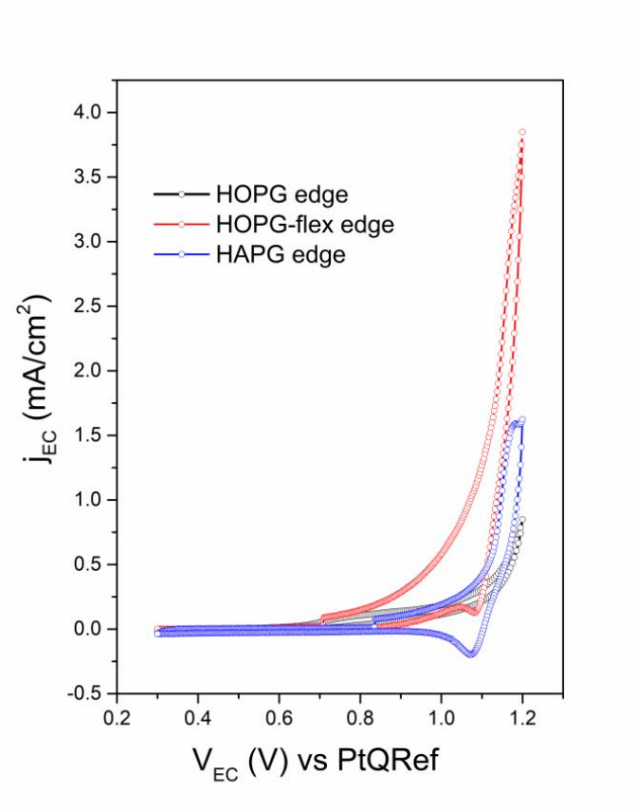

Figure 13. CV of the "edge-samples" sample. Scan rate = 25 mV/s.

ii) INFN samples

Another interesting study-case consists of GNPs buckypaper (see the Materials and Metods paragraph for details). In **Figure 14**, we show the voltammogram acquired on such sample.

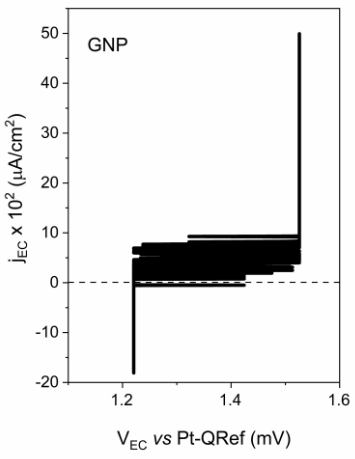

Figure 14. CV of the GNPs buckypaper sample. Scan rate = 25 mV/s.

As reported in the figure, no clear peaks or features along the CV cycle are observed. In this case, the Faradaic current cuts the whole range of the amperometer within a very small EC potential interval. The preparation procedure for the sample

together with a large amount of defects (the sample is obtained after a mechanical preassure load) can explain this result. From this CV, we deduce that no blisters affect the electrode surface as proved in **Figure 15**.

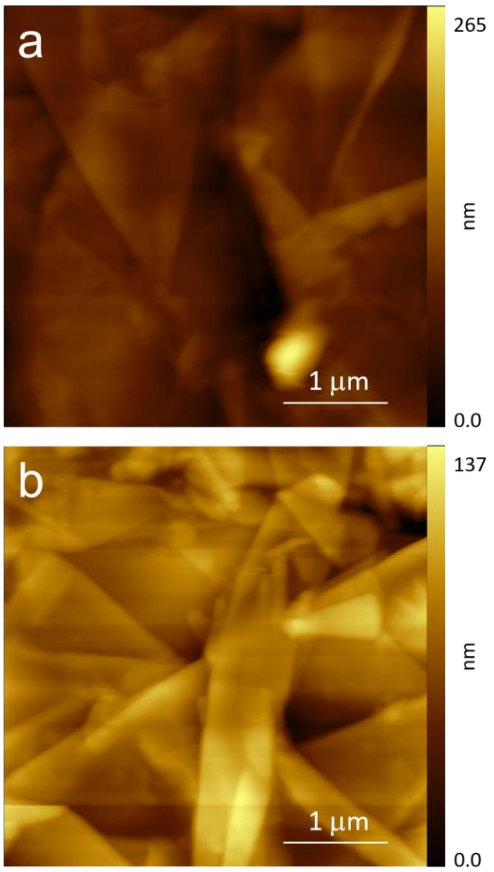

Figure 15. AFM topography images of GNPs buckypaper. a) pristine sample, b) post EC acid-treatment.

In this case, the flat regions are not as wide as in Figure 12. However, considering the morphology and the differences in height between these samples, we believe that the electrode surface is rich in defects and holes, where the electrolyte can easily penetrate inside the sample. By comparing these results to the one obtained for the TPG specimens, we can clearly rule out that, changing the electrode density by tuning the pressure load during the sample preparation, cavities, holes, defects by which the electrolyte intercalates inside the sample significantly influence the current density. The numerous holes represent instead preferential gates for the gas output produced during the anion intercalation. This gives a rationale for the lack of blisters in these samples.

i) Other carbon forms

Glassy carbon is widely used in electrochemistry and in industrial application due to its mechanical properties (not exfoliable, good physical and chemical stability, well-finished surface). **Figure 16** shows a CV acquired with the glassy carbon electrode. The CV presents characteristics of an almost ideal working electrode: there are no features, the OER is clearly visible and the Faradaic current increases its intensity while the EC potential is changed towards positive values. The electrode stability, the high-quality CV, the absence of any feature related to the solvated anion intercalation suggests that no blisters could affect the glassy carbon surface.

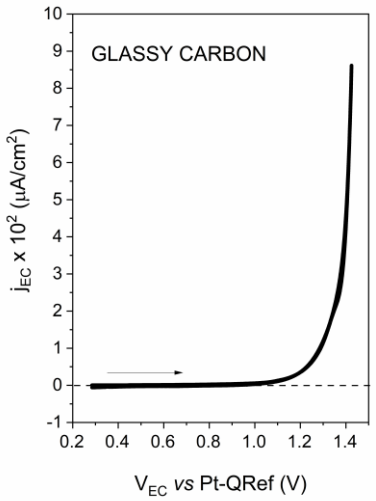

Figure 16. CV of the glassy carbon sample. Scan rate = 25 mV/s.

In **Figure 17**, we report the morphological analysis.

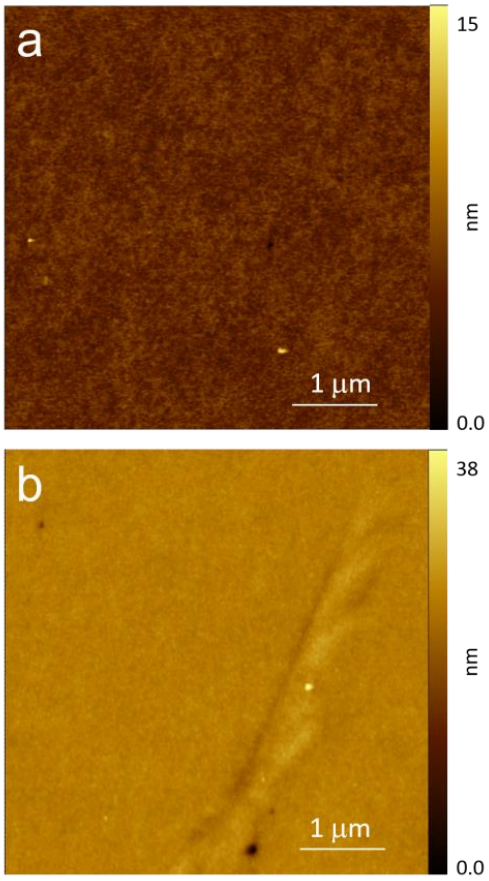

Figure 17. AFM topography images of glassy carbon. a) pristine sample, b) post EC acid-treatment.

No terraces and steps are visible in panel a. The surface is quite flat (as evident from the color scale). After the EC treatment, no blisters affect the surface morphology, in agreement with our prediction based on the CV analysis. On the AFM length-scale, it is possible to observe some defects on the surface as that one reported in panel b. We speculate that the relative high EC potential used in the experiment, together with the electrolyte molarity selected for this experiments, can locally affect the sample surface, creating defects. Consequently, it is possible that, if glassy carbon is used for a long time, the surface undergoes a significant detriment, leading to an enhancement of its roughness. However, we do not believe that this progressive surface detriment could cause the basal plane swelling. In fact, blister growth consists in an intercalation inside a stratified bulk structure and GIC formation that is not possible with the glassy carbon structure.

Since the high surface roughness makes the AFM acquisition very difficult to carry out, pyrolitic graphite will be studied only by electrochemistry. In **Figure 18**, we show the acquired CV, which presents some peculiarities.

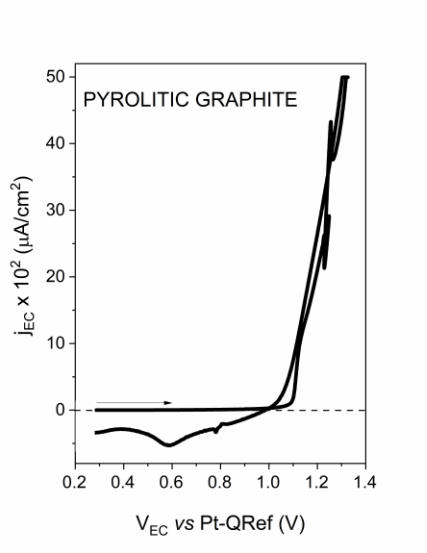

Figure 18. CV of the pyrolitic graphite sample. Scan rate = 25 mV/s.

the first part of the voltammogram seems to mimic the glassy carbon electrode reported in Figure 16. However, during the Faradaic current enhancement, some instabilities are observed: the current density maximum reaches the amperometer saturation and, in the cathodic regime, some features appear. The latter are similar to those observed in the HOPG CV related to the anion de-intercalation process. We speculate that, when high positive potentials are reached during the scan, the electrode undergoes an intense carbon dissolution. On the one hand, this causes the current density to increase; on the other hand, it creates defects and holes for the anion intercalation inside the electrode bulk. The absence of an ordered stratified structure suggests that blisters should not evolve on this electrode. In any case, blisters as those reported in Figure 1 could be hidden by the high surface roughness.

Lastly, carbon foam results to be another sample that cannot be investigated by AFM. The collected CV (see **Figure 19**) is interesting compared to the other carbon forms reported above. The maximum current intensity is not very high compared with the CV related to the pyrolitic graphite (Figure 18). This is probably due to the fact that carbon foam presents a very low density with respect to the previous samples.

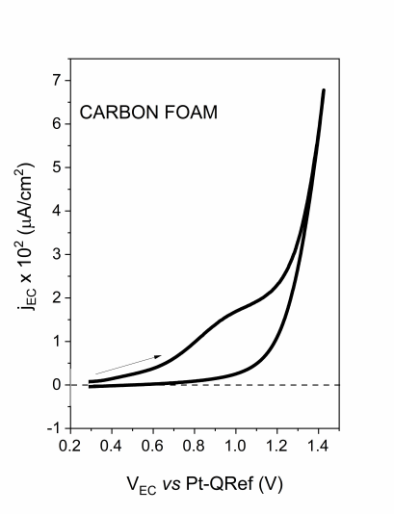

Figure 19. CV of the pyrolitic graphite sample. Scan rate = 25 mV/s.

The peak at around 0.9 V is superimposed to the exponential growth due to the oxygen evolution. This feature has a different shape but the EC potential value is close to the IV HOPG intercalation stage. Probably, the electrode undergoes similar chemical reactions as those related to eq.1. Being a foam (gas cannot be entrapped inside the electrode) we do not observe any de-intercalation feature during the cathodic sweep.

4. Conclusions

The comparison among various PGs shows that the material structure of graphites plays a key role in redox reaction of the electrochemical cell. Nevetheless, it is rather difficult to give a simple explanation for the role of the defects in such reactions. Indeed, intercalation is a comlex process consisting of a several steps, each potentially rate limiting.

Intercalation usually starts at the edge of crytsallites. On the contrary, due to pecuiliarities of PG samples, the intercalate is more often in contact with the basal-plane surface of the sample. Thus, to start the reaction, the anions must first diffuse into the sample, and many researches noted [40, 42] that the penetration sites are likely grain boundaries, microcracks and atomic steps on the surface.

In HOPG, commonly used for studying the intercalation process, grain boundaries accompanied by wide defect regions observed under the acustic microscope [39] can be such penetration paths. Thus, in HOPG, intercalation is minimally limited by diffussion of the intercalate from the basal-plane into the sample .

In HOPG-flex and HAPG, the grain boundary is quite perfect [40], and the intercalation is severely limited by the need to diffuse the agent (*e. g*., anions, sovated ions) into the sample and reach the intercalation points. It seems that, for these two materials under the conditions in our experiments, intercalation occurs mainly in the atomic steps on the basal-surface . This is confirmed by the observed blister formation predominantly near the edge of steep steps. Furthermore, blisters can appear at the most defective areas of the grain boundary, for example, at a triple junction of the grain boundaries, as can be seen in Figure 6. We assume that this explains why only the very first intercalation/deintercalation run is observed in HOPG-flex

Accoding to [40,43], the number and the height of atomic steps on the basal surface in HAPG is even much smaller than in HOPG-flex, the grains are several times larger, and the grain boundary is ideal. Therefore, in HAPG, under given experimental conditions, the intercalation reaction is missed compared to the simple carbon oxidation reaction.

For edge samples, the intercalate is in direct contact with the edges of crystallites, and only the defects within the crystallites affect the reaction.

A direct measurement of defects in various PG [40] reveals a greater number of interlayer defects in HOPG compared to HOPG-flex, which may explain the lower intercalation activity of HOPG sample compared to HOPG-flex and HAPG, providing that diffusion of the intercalate into the sample does not limit the reaction. An interlayer defect binds adjacent carbon layers, and this bond must be broken for the intercalate inserting into interlayer space. Thus, more perfect structures are more easily intercalated by anions, as was mentioned by many reseachers [32,44]

According to [40], HAPG has a minimum of defects, and should present an even easier intercalation than the one expected for HOPG-flex. However, this is not the case. A possible explanation might be the presence of much larger grains in HAPG compared to other materials. Those grains lead to slower diffusion of the intercalate into the grains themselves, which are additionally suppressed by the stress caused by deformation of the carbon layers between the intercalated and clean areas.

The results show that the intercalation reaction is very sensitive to the structure of graphite material. The structural features, as well as the alignment of the structural element within the sample, can change the rate of the number of steps and the behavior of graphite material as an electode in an electrochemical cell.

Acknowledgements

The wide research activity reported in this work was possible thanks to the help of and interaction with many people. The authors are gratefull to A. Li Bassi, C. S. Casari, C. Castiglioni, M. Tommasini, L. Brambilla (Politecnico di Milano), S. Bistarelli (INFN – Laboratori Nazionali di Frascati) for useful discussion.

References

[1] Fan L, Liu Q, Chen S, Lin K, Xu Z and Lu B 2017 *Small* **13** 1701011

[2] Yao KPC, Okasinski JS, Kalaga K, Shkrob IA and Abraham DP 2019 *Energy Environ. Sci.* **12** 656

[3] Yivlialin R, Bussetti G, Penconi M, Bossi A, Ciccacci F, Finazzi M and, Duò L 2017 *ACS App. Mater. Inter.* **9**(4) 4100

[4] Yi Y, Weinberg G, Prenzel M, Greiner M, Heumann S, Becker S and Schlögl R 2017 *Catalysis Today* **295** 32

[5] Wang J, Yang B, Zhong J, Yan B, Zhang K, Zhai C, Shiraishi Y, Du Y and Yang P 2017 *J. Coll. Interf. Sci.* **497** 172

[6] Wu Y, Deng P, Tian Y, Ding Z, Li G, Liu J, Zuberi Z and He Q 2020 *Bioelectrochem* **131** 107393

[7] Bai M, Wu W, Meng Y and Liu L 2020 *Chem. Eng. Processing – Process Intensification* **149** 107839

[8] Lin Y, Chen R, Zhang Y, Lin Z, Liu Q, Liu J, Wang Y, Gao L and Wang J 2020 *Materials & Design* **186** 108304

[9] Tsang CHA, Huang H, Xuan J, Wang H and Leung DYC 2020 *Renew. Sustain. En. Rev.* **120** 109656

[10] Ismail AF, Goh PS, Sanip SM and Aziz M 2009 *Sep. Pur. Technol.* **70** 12

[11] Qian D, Wagner GJ, Liu WK, Yu MF and Ruoff RS 2002 *Appl. Mech. Rev.* **55** 495

[12] Sinha N and Yeow JYW 2005 *IEEE Transactions on NanoBioscience* **4** 180

[13] Inomata K, Kanazawa K, Urabe Y, Hosono H and Araki T 2002 *Carbon* **40** 87

[14] Kim J, Hwan Kwon O, Kang YH, Jang KS, Cho SY and Yoo Y 2017 *Compos. Sci Technol.* **153** 32

[15] Huang SY, Li Q, Zhu Y and Fedkiw PS 2017 *J. Appl. Electrochem.* **47** 105

[16] Farhan S, Wang R and Li K 2016 *J. Mater. Sci* **51** 7991

[17] Wang Y, Serrano S and Santiago-Avilés JJ 2003 *Symth. Metals* **138** 423

[18] Estrade-Szwarckopf H 2004 *Carbon* **42** 1713

[19] Cao A, Xu C, Liang J, Wu D and Wei B 2001 *Chem. Phys. Lett.* **344** 13

[20] Gallagher MJ, Chen D, Jacobsen BP, Sarid D, Lamb LD, Tinker FA, Jiao J, Huffman DR, Seraphin S and Zhou D 1993 *Surf. Sci.* **281** L335

[21] Bleda-Martínez MJ, Lozano-Castelló D, Morallón E, Cazorla-Amorós D and Linares-Solano A 2006 *Carbon* **44** 2642

[22] Vidu R, Quinlan FT and Stroeve P 2002 *Ind. Eng. Chem. Res.* **41** 6546

[23] Sugita S, Abe T and Itaya K 1993 *J. Phys. Chem.* **97** 8780

[24] De Rosa S, Branchini P, Yivlialin R, Duò L, Bussetti G and Tortora L 2020 *ACS Appl. Nano Mater*. **3** 691

[25] Bussetti G, Yivlialin R, Goletti C, Zani M and Duò L 2019 *MDPI Condens. Matter* **4**, 23

[26] Yivlialin R, Bussetti G, Magagnin L, Ciccacci F and Duò L 2017 *Phys. Chem. Chem. Phys*. **19** 13855

[27] Yivlialin R, Magagnin L, Duò L and Bussetti G 2018 *Electrochimica Acta* **276** 352

[28] Bussetti G, Yivlialin R, Alliata D, Li Bassi A, Castiglioni C, Tommasini M, Casari CS, Passoni M, Biagioni P, Ciccacci F and Duò L 2016 *J. Phys. Chem. C* **120** 6088

[29] Yivlialin R, Bussetti G, Brambilla L, Castiglioni C, Tommasini M, Duò L, Passoni M, Ghidelli M, Casari CS and Li Bassi A 2017 *J. Phys. Chem. C* **121** 14246

[30] Pavoni E, Yivlialin R, Hardly Joseph C, Fabi G, Mencarelli D, Pierantoni L, Bussetti G and Farina M 2019 *RCS Adv.* **9** 23156

[31] Yivlialin R, Brambilla L, Accogli A, Gibertini E, Tommasini M, Goletti C, Leone M, Duò L, Magagnin L, Castiglioni C and Bussetti G 2020 *Appl. Surf. Sci.* **504** 144440

[32] Dresselhaus MS and Dresselhaus G 2002 *Adv. Phys*. **51** 1

[33] Goss CA, Brumfield JC, Irene EA and Murray RW 1993 *Anal. Chem*. **65** 1378

[34] Alliata D, Häring P, Haas O, Kötz R and Siegenthaler H 1999 *Electrochem. Comm*. **1** 5

[35] Inzelt G 2013 Pseudo-reference Electrodes. In: Inzelt G., Lewenstam A., Scholz F. (eds) Handbook of Reference Electrodes. Springer, Berlin, Heidelberg

[36] Bellucci S, Bovesecchi G, Cataldo A, Coppa P, Corasaniti S and Potenza M 20 19 *Materials*, **12**(5), 696

[37] Maffucci A, Micciulla F, Cataldo A, Miano G and Bellucci S 2016 *Nanotechnology* **27**(9) 095204

[38] Dabrowska A, Bellucci S, Cataldo A, Micciulla F and A Huczko 2014 *Phys. Status Solidi B*, **251**, 1–4

[39] Grigorieva Iand Antonov A 2003 *X-Ray Spectrom.*, **32**, 64–68

[40] Sinitsina O, Meshkov G, Grigorieva A, Antonov A, Grigorieva I and Yaminsky I 2018 *Beilstein J. Nanotechnol.***,** **9**, 407–414

[41] Grigorieva I, Antonov A and Gudi G 2019 *Condens. Matter*, **4**, 18

[42] Eklund PC, Olk CH, Holler FJ, Spolar JG and Arakawa E T 1986 *J. Mater. Res.***, 1**, 361–367.

[43] Sinitsyna O, Ahmetova A, Meshkov G, Goncharova T, Pylev I, Smirnova M, Belov Yuand Yaminsky I , 2018 *Nano Indusrty*, **2**(81), 170-172

[44] Anderson Axdal SH and Chung DDL 1987 *Carnbon*, **25**(3), 377-398